ELSEVIER

Journal of Power Sources 79 (1999) 277–280

JOURNAL OF POWER SOURCES

Short communication

Cyclic voltammetric studies of stabilized α-nickel hydroxide electrode

Liu Bing *, Yuan Huatang, Zhang Yunshi, Zhou Zuoxiang, Song Deying

Institute of New Energy Material Chemistry, Nankai University, Tianjin 300071, China

Received 25 November 1998; accepted 2 January 1999

Abstract

Substitution of aluminum for nickel in the lattice of nickel hydroxide, prepared by co-precipitation, leads to hydrofalcite-like compound of α-nickel hydroxide. This compound has been used as the electrochemical active material in the positive electrodes of rechargeable alkaline batteries. Cyclic voltammetric studies suggest that α-nickel hydroxide displays better reversibility of the $Ni(OH)_2$/NiOOH redox couple. The mechanism of the electrode reaction is still found to be controlled by proton diffusion, and the proton diffusion coefficient differs with the content of aluminium. © 1999 Elsevier Science S.A. All rights reserved.

Keywords: Nickel hydroxide electrode; Cyclic voltammetry; Reversibility; Proton diffusion coefficient

1. Introduction

Nickel hydroxide has been widely used as the positive active-material in rechargeable alkaline batteries [1–3]. Usually, the β-(II)/β-(III) phase is the chemical material involved during electrode cycling. The α/γ couple is known, however, to exhibit better electrochemical properties than the β-(II)/β-(III) couple [4]. Unfortunately, α-$Ni(OH)_2$ reverts to β-$Ni(OH)_2$ on standing in alkaline media. Recently, in order to increase the specific energy of nickel/cadmium and nickel/metal hydride batteries, a high-performance pasted nickel electrode made from a porous foam nickel or fibrous nickel substrate has been developed. Much research work has been performed to stabilize α-$Ni(OH)_2$ [5,6], e.g., by doping with trivalent cations.

In our previous studies, the synthesis of aluminium stabilized α-$Ni(OH)_2$ by chemical co-precipitation has been developed [7]. In the present study, the electrochemical characteristics of the α-$Ni(OH)_2$ electrode are investigated by cyclic voltammetry, and the reversibility of the $Ni(OH)_2$/NiOOH redox reaction is examined. In addition, the reasons for the high performance of α-$Ni(OH)_2$, are discussed.

2. Experimental

2.1. Preparation of samples

α-$Ni(OH)_2$ substituted with aluminium was prepared according to the method reported previously [7].

2.2. Physical characterization

The structure was determined using X-ray diffraction (XRD) (D/Max-IIIA X-ray diffractometer, Rigaku, Japan), CuKα radiation and a nickel filter at 35 kV and 40 mA.

2.3. Electrochemical characterization

All cyclic voltammetric studies were performed in a three-compartment electrolysis cell at 25°C using an EG and G PARC Model 273 potentiostat/galvanostat and M270 electrochemical analyzing system with a personal computer. The working electrodes were powder microelectrodes with diameters of 150 μm. Two nickel sheet counter electrodes were placed on either side of the working electrode. A Hg/HgO reference electrode was used with a Luggin capillary in the region of the working electrode. All potentials are reported with respect to this reference electrode. The working electrodes were activated by repeated potential scanning between 0 and 0.7 V at the 10 mV/s rate for 10 times prior to the experiments.

* Corresponding author. Fax: +86-222350-2604; E-mail: bingliu@tju.edu.cn

0378-7753/99/$ - see front matter
PII: S0378-7753(99)00053-1

3. Results and discussion

The powder XRD patterns of $Ni(OH)_2$ samples with different aluminium content are shown in Fig. 1. All the samples with different aluminium content exhibited the typical characterization of α-$Ni(OH)_2$. α-$Ni(OH)_2$ and β-$Ni(OH)_2$ crystallize as a hexagonal system with the brucite-type structure and with $Ni(OH)_2$ layers stacked along the *C*-axis. Each $Ni(OH)_2$ layer consists of a hexagonal planar arrangement of octahedrally oxygen coordinated Ni(II) ions. The main difference between α-$Ni(OH)_2$ and β-$Ni(OH)_2$ resides in the stacking of the layers along the *C*-axis. β-$Ni(OH)_2$ layers are perfectly stacked along the *C*-axis with an interlamellar distance of 4.6 Å, but α-$Ni(OH)_2$ layers are randomly oriented and separated by intercalated water molecules bonded to the hydroxyl groups by hydrogen bonds. The interlamellar distance for the α-$Ni(OH)_2$ is about 8 Å. The XRD pattern of aluminum stabilized α-$Ni(OH)_2$ is the same as that of unsubstituted α-$Ni(OH)_2$ as reported in literature [8,9]. The XRD pattern of stabilized α-$Ni(OH)_2$ in Fig. 1 displays a low angle reflection close to 8 Å, followed by another at around 4 Å. The results are in agreement with values found by Kamatt et al. [10] and Indira et al. [11] for the layered double hydroxides (LDHs) of nickel with aluminum. In addition, the pattern shows a pronounced asymmetry towards the 0.27–0.23 nm region due to the (hk0) reflections, a feature which is characteristic of a turbostratic structure.

Cyclic voltammograms for electrodes with different aluminium contents are given in Fig. 2. Only one anodic oxidation peak for the electrode with 10 wt.% Al (at about 504 mV) was recorded prior to oxygen evolution. Similarly, only one oxyhydroxide reduction peak at about 361 mV was observed on the reverse sweep. Similar voltammograms were observed for an electrode with a higher aluminium content (25 wt.% Al), but the anodic peak corresponding to nickel hydroxide oxidation and the cathodic peak corresponding to nickel oxyhydroxide reduction shift to more positive potentials, compared with those of the electrode with 10 wt.% Al.

In order to compare the characteristics of the electrodes, the results of the cyclic voltammetric study in Fig. 2 are tabulated in Table 1. The average peak potential, E_{rev}, is taken as an estimate of the reversible potential and the difference in the anodic and cathodic positions, $\Delta E_{a,c}$, is taken as an estimate of the reversibility of the redox reaction [12,13]. Oxygen evolution is a parasitic reaction during charging of the nickel electrode. To compare the effect of stabilized α-$Ni(OH)_2$ on the oxygen evolution reaction, the difference between the oxidation peak potential and the oxygen evolution potential (DOP) [14] on the return sweep required to produce 1.5×10^{-5} A of anodic current is also estimated from the voltammograms. The results of the cyclic voltammetric studies in Fig. 2 are tabulated in Table 1 in comparison with β-$Ni(OH)_2$ [15].

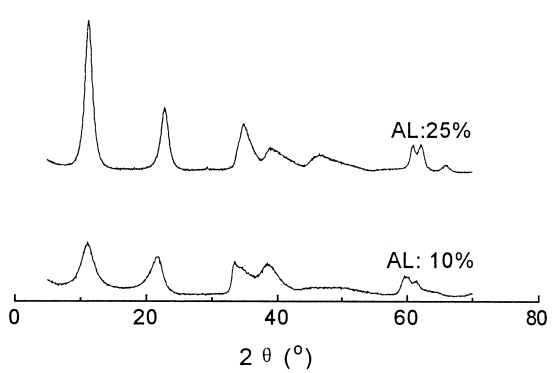

Fig. 1. XRD patterns of α-nickel hydroxide.

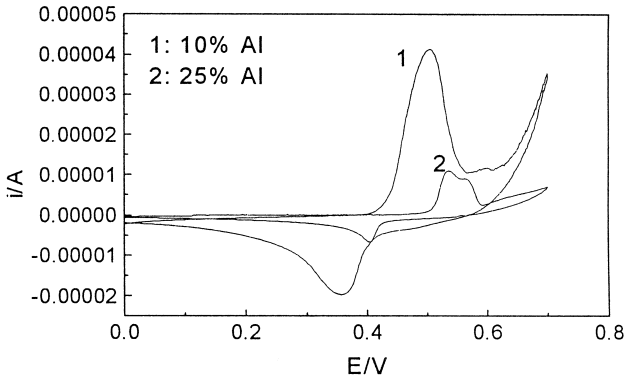

Fig. 2. Cyclic voltammograms for (1) electrode with 10 wt.% Al; (2) electrode with 25 wt.% Al. Scan rate: 0.5 mV s^{-1}.

The data in Table 1 illustrate that nickel hydroxide with 25 wt.% Al content allows the charge process to occur more reversibly than that with 10 wt.% Al (ΔE_p is 132 mV instead of 143 mV). Moreover, Al substituted α-$Ni(OH)_2$ displays a better reversible charge process than β-$Ni(OH)_2$ with cobalt coating on the surface (ΔE_p is 132 mV instead of 280 mV). In addition, the oxygen evolution overpotential shifts to a more positive value. Thus, these results indicate clearly that aluminum stabilized α-$Ni(OH)_2$ electrode allows the charge process to occur more easily and more reversibly, and suggests that much more active material can be utilized during charge. Besides, due to the increase in the oxygen evolution overpotential and the decrease of the oxidation peak potential of nickel hydroxide, the charge efficiency of the electrode can be markedly improved, which indicates that the electrode has greater

Table 1
Results of cyclic voltammetry measurements

Electrode	E_a (mV)	E_c (mV)	$\Delta E_{a,c}$ (mV)	E_{rev} (mV)	DOP (mV)
1	504	361	143	432	155
2	537	405	132	471	92
3	520	240	280	380	89

(1) Aluminum stabilized α-$Ni(OH)_2$ (Al: 10 wt.%).
(2) Aluminum stabilized α-$Ni(OH)_2$ (Al: 2 wt.%).
(3) β-$Ni(OH)_2$ microencapsulated by 5 wt.% Co [14].

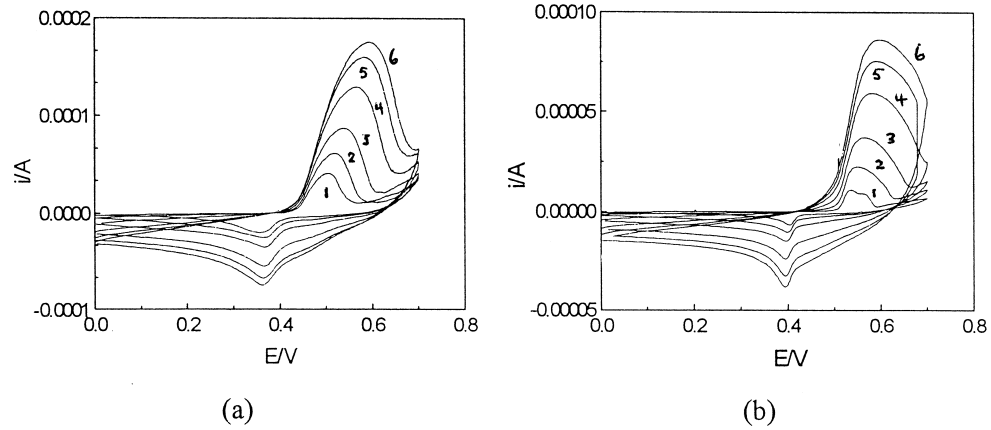

Fig. 3. Cyclic voltammograms for electrodes with: (a) 10 wt.% Al; (b) 25 wt.% Al. (1) 0.5 mV s^{-1}; (2) 1 mV s^{-1}; (3) 2 mV s^{-1}; (4) 5 mV s^{-1}; (5) 8 mV s^{-1}; (6) 10 mV s^{-1}.

discharge capacity. These results are in good agreement with those obtained by Corrigat and Bendert [13], who have reported that co-precipitation of cobalt or manganese in nickel hydroxide thin films decrease the oxidation potential compared with that of unsubstituted nickel hydroxide.

Typical cyclic voltammograms for nickel hydroxide with different aluminium content at various scan rates are shown in Fig. 3. As the scan rate increases, the anodic peak potential and the cathodic peak potential both shift in a more positive direction. The characteristic cyclic voltammetric parameters obtained from Fig. 3 are shown in Fig. 4 as a function of sweep rate. It can be seen from Fig. 4 that the peak current i_{pa} vs. $V^{1/2}$ plot, where V is the voltage scan rate, gives a reasonable linear relationship, while i_{pa} vs. V does not give a linear relationship. In semi-infinite diffusion controlled cyclic voltammetry in liquid electrolytes, i_{pa} vs. $V^{1/2}$ gives a linear relationship regardless of scan rate for a kinetically uncomplicated redox reaction; for an adsorption process, i_{pa} vs. V is expected to be linear at different rates. In the present study, the linear relationship between i_{pa} and $V^{1/2}$ suggests that the oxidation of nickel hydroxide is diffusion limited, as noted by other authors [16,17].

In the case of semi-infinite diffusion, the peak current i_p may be expressed by the classical Sevick equation [18]:

$$i_p = 2.69 \times 10^5 n^{3/2} A D_o^{1/2} V^{1/2} C_o \quad (1)$$

where n is the number of electrons transferred; A is the apparent surface area of the electrode; D_o is the diffusion coefficient of the rate limiting species, i.e., proton; C_o is the proton concentration. To estimate the proton concentration in the nickel hydroxide, it is assumed to be the same as that of $Ni(OH)_2$ from the stoichiometry of the reaction [19]:

$$Ni(OH)_2 \rightarrow NiOOH + H^+ + e^- \quad (2)$$

The concentration of $Ni(OH)_2$ is estimated by dividing the molecular weight of α-$Ni(OH)_2$ by its density, 2.82 g cm^{-3} [20]. According to Eq. (1) and the slope of i_{pa} vs. $V^{1/2}$ in Fig. 4, it is calculated that the proton diffusion coefficient in nickel hydroxide with 10 wt.% Al is 1.1×10^{-8} cm^2 s^{-1}, and that with 25 wt.% Al is 3.21×10^{-9} cm^2 s^{-1}. Zhang and Park [19] reported a diffusion coeffi-

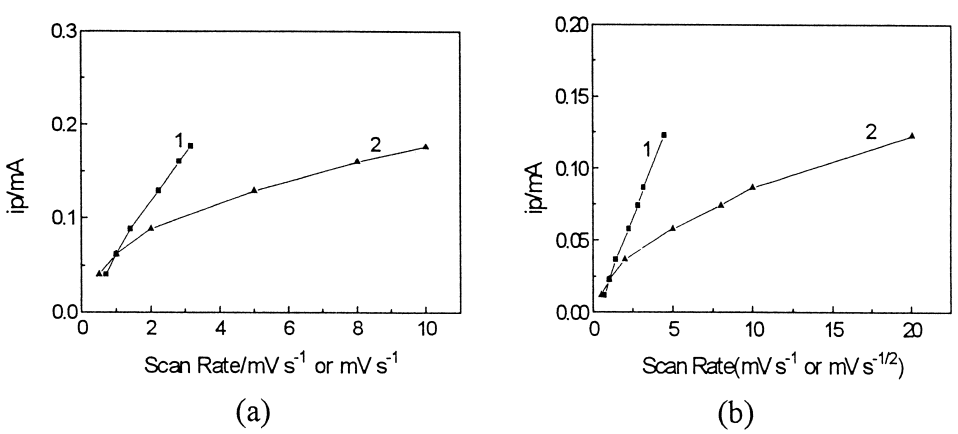

Fig. 4. Variation of anodic peak current with scan rate for electrodes with: (a) 10 wt.% Al; (b) 25 wt.% Al. (1) i_p–$V^{1/2}$; (2) i_p–V.

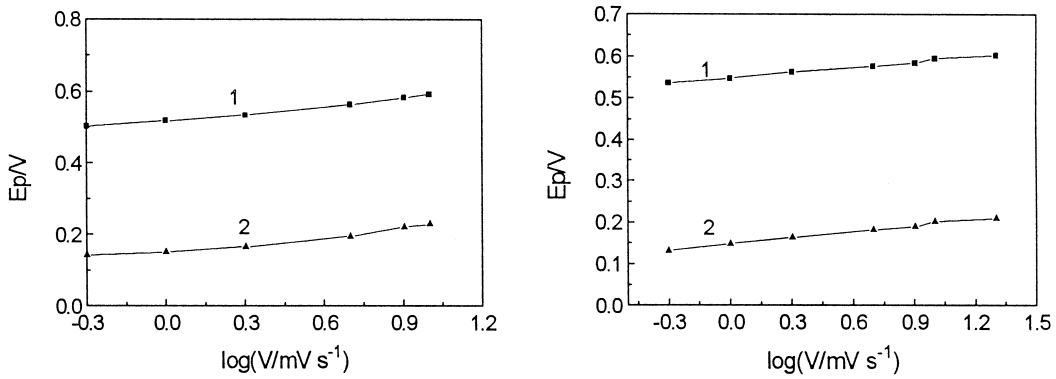

Fig. 5. Variation of E_{pa} and ΔE_p with scan rate for electrodes with (a) 10 wt.% Al; (b) 25 wt.% Al. (1) E_p–log(V); (2) ΔE_p–log(V).

cient of 1.0×10^{-11} cm^2 s^{-1} for β-Ni(OH)$_2$ from cyclic voltammetry. This value is considerably smaller than the present value.

The potentials of the current peaks in Fig. 3 change linearly with log(V) (Fig. 5), which has also been observed by Guzman et al. [17]. But as seen from Fig. 5, the magnitude of the change is very small. This indicates that the same process is taking place at all scan rates. The difference (ΔE) between E_{pa} and E_{pc} is fairly constant at low scan rates, and generally increases at high scan rate. Thus, on the basis of liquid electrolyte reversibility criteria, the reaction approaches reversibility only at low scan rates. Of course, since no attempt was made at iR compensation, increases of ΔE_p observed at higher scan rates may be due to greater uncorrected potential differences at higher scan currents. As a general rule, however, the aluminum substitute α-nickel hydroxide electrode has the same kinetic mechanism as the β-nickel hydroxide electrode.

4. Conclusions

(1) Aluminum stabilized α-Ni(OH)$_2$ has the same structure as that of α-Ni(OH)$_2$.

(2) The electrode reactions occurring at aluminum stabilized α-Ni(OH)$_2$ display better redox reversibility, and the oxygen evolution overpotential shifts more positive value.

(3) Due to the insertion of anions in the interslab, the electrode has a relatively higher proton conductivity. The presence of aluminum in the nickel hydroxide does not change the kinetic mechanism of the electrode reaction and modifies the proton conductivity of the nickel hydroxide. The electrode reaction is still found to be controlled by proton diffusion and the proton diffusion coefficient is 1.1×10^{-8} cm^2 s^{-1} for 10 wt.% Al and 3.2×10^{-9} cm^2 s^{-1} for 25 wt.% Al.

(4) Aluminum stabilized α-Ni(OH)$_2$ has better electrochemical activity and is a candidate electrode material for alkaline secondary cells.

References

[1] A.K. Sood, J. Appl. Eletrochem. 16 (1986) 274.
[2] M.E. Unates, M.E. Folquer, J.R. Vilche, A.J. Arvia, J. Electrochem. Soc. 139 (1992) 2697.
[3] Y.J. Kim, S. Srinivasan, A.J. Appleby, J. Appl. Electrochem. 20 (1990) 377.
[4] L. Indria, M. Dixit, P. Vishnu, J. Power Sources 52 (1994) 93.
[5] P.V. Kamath, M. Dixit, L. Indrin, J. Electrochem. Soc. 141 (1994) 2956.
[6] M. Dixit, P.V. Kamath, J. Power Sources 56 (1995) 97.
[7] L. Bing, W. Xianyou, Y. Huantang, J. Appl. Electrochem. (in press).
[8] P. Oliva, J. Leohardi, J.F. Lauvent et al., J. Power Sources 8 (1982) 229.
[9] M.C. Bernard, P. Vernard, M. Keddam et al., Electrochim. Acta 41 (1996) 91.
[10] P.V. Kamath, M. Dixit, L. India et al., J. Electrochem. Soc. 141 (1994) 2956.
[11] L. Indira, M. Dixit, P.V. Kammath, J. Power Sources 52 (1994) 93.
[12] P.V. Kamath, M.F. Ahmed, J. Appl. Electrochem. 23 (1993) 225.
[13] D.A. Corrigan, R.M. Bendert, J. Electrochem. Soc. 136 (1989) 72.
[14] X.Y. Wang, J. Yan, Y.S. Zhang, J. Power Sources 72 (1998) 221.
[15] X.Y. Wang, J. Yan, Y.S. Zhang, J. Appl. Electrochem. (in press).
[16] D.M. MarArthur, J. Electrochem. Soc. 117 (1970) 729.
[17] R.S.S. Guzman, J.R. Vilche, A.J. Arvia, J. Electrochem. Soc. 125 (1978) 1578.
[18] Southampton Electrochemistry Group, Instrumental Methods in Electrochemistry, Ellis Horwood, England, 1985.
[19] C. Zhang, S.M. Park, J. Electrochem. Soc. 134 (1987) 2966.
[20] M. Oshitani, T. Takayama, K. Takashima, J. Appl. Electrochem. 16 (1986) 403.